HYGRID

FLEXIBLE HYBRID SEPARATION SYSTEM FOR H2 RECOVERY FROM NG GRIDS

FCH-2 GRANT AGREEMENT NUMBER: 700355

Start date of project: 01/05/2016 **Duration: 3 years**

WP6 – Lab scale testing

D.6.2
Results on membranes and sorbents

Topic: Development of technology to separate hydrogen from low-concentration hydrogen streams
Funding scheme: Research and Innovation Action
Call identifier: H2020-JTI-FCH-2015-1

Due date of deliverable: 31-12-2017	Actual submission date: 03-04-2018	Reference period: 01-05-2016 – 31-12-2017
Document classification code (*): HYGRID-WP6-D62-01032018-version0.1.ext		Prepared by (**): Maria Nordio (TUE)

Version	DATE	Changes	CHECKED	APPROVED
v0.1	29-03-18	First Release	TUE	FAUSTO GALLUCCI
V0.2	03-04-2018	Second release	TUE	SW

Project funded by the FCH-2 JU within the H2020 Programme (2014-2020)		
Dissemination Level		
PU	Public	X
PP	Restricted to other programme participants (including the Commission Services)	
RE	Restricted to a group specified by the consortium (including the Commission Services)	
CO	Confidential, only for members of the consortium (including the Commission Services)	
CON	Confidential, only for members of the Consortium	

(*) for generating such code please refer to the Quality Management Plan, also to be included in the header of the following pages

(**) indicate the acronym of the partner that prepared the document

Content

1. EXECUTIVE SUMMARY

1.1. Description of the deliverable content and purpose

This document aims to describe the experimental results obtained with membranes and sorbents, tested at different operating conditions. The main purpose is to verify hydrogen recovery factor and purity of different types of membrane, tested at the conditions of HyGrid project. The mixture fed is equal to 10% H_2 and 90% CH_4 at different pressures and 400 ºC.

1.2. Brief description of the state of the art and the innovation brought

The main task of the D6.2 is the description of membrane and sorbent results. Different types of membranes have been tested at the operating conditions of Hygrid project. A model for the simulation of the membrane has been developed in order to describe and predict the experimental results. The model includes mass transfer limitation in the retentate side and in the porous support. For the mass transfer in the retentate side a Sherwood correlation from literature has been included while for the porous support, the dusty gas model was considered.

1.3. Deviation from objectives

There are no deviations.

1.4. If relevant: corrective actions

There are no deviations.

1.5. If relevant: Intellectual property rights

2. INTRODUCTION

Main drivers for a sustainable energy visions of the future of the world on the need to:

1. Reduce global emissions
2. Ensure security of energy supply
3. Create a new industrial and technology energy base crucial for our economic prosperity

Hydrogen is an attractive alternative to fossil fuels. Some of the main attraction of hydrogen gas is that it can be produced from different resources, both renewable and non-renewable. Hydrogen can then be utilized in high-efficiency power generation system, in fuel cells for vehicular transportation and electricity generation. One of the main problem related to the traditional power plants is the great exergetic losses due to the mechanical conversions. To overpass the modern efficiencies of the traditional conversions systems it is necessary to avoid the conversion process based on the combustion of the fuel. Since the fuel cell allow the direct conversion of chemical energy in electricity, they are one of the promising systems that could reach higher efficiencies.

3. SETUP

The setup for testing the membranes consists of 5 mass flow controllers up to 5 l/min for feeding the inlet gases, such as H_2, CH_4, He, N_2 and air; an oven for heating up the membrane; a reactor in which the membrane is installed; a pressure controller for the retentate side in order to maintain the operating pressure required.

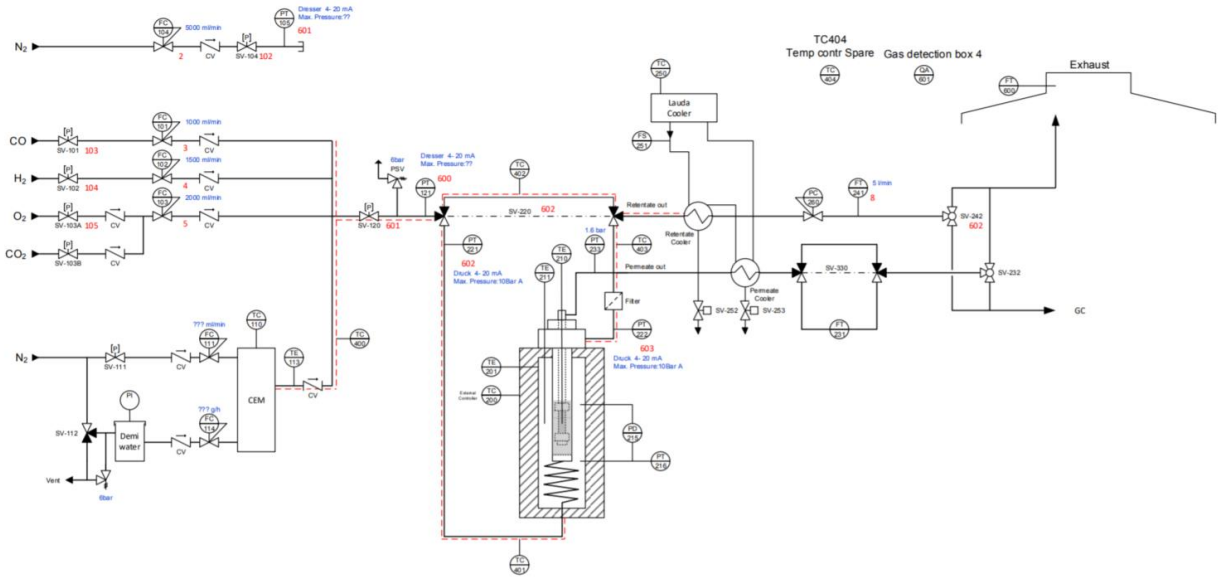

Figure 1. Schematic description of the membrane test setup

A schematic representation of the setup is depicted in Figure 2. Different mass flow controllers, supplied by Brooks Instruments, regulate process gases and permeate feed flow in the working range between 0-5 L/min. The inlet gases to be fed are H_2, N_2, He and CH_4. The inlet gases are heated up in a cylindrical reactor with a diameter of 4.2 cm and a length of 42.3 cm. The membrane is attached to the flange of the reactor and it is located in the middle of the reactor. Process gases are fed to the shell side of the membrane while a counter-current sweep gas is fed to the lumen side of the membrane. The permeate side is at atmospheric pressure while, the inlet of the retentate side is regulate through a back pressure regulator supplied by Bronkhorst, which allow to control the pressure up to 5 bar. The reactor is placed in an electrically heated oven where the membrane and the process gases are heated up to the operating temperature. Two thermocouples are located in the retentate and permeate side of the membrane to measure the temperature of the system. An acquisition and control system regulates the main process parameters such as temperature and pressure, interfaced with a computer. A soup bubble flow meter Horibastec has been used for the pure gas measurements and a micro-GC Agilent model for analysing the mixture with and without sweep gas in order to evaluate the hydrogen purity.

4. MEMBRANE TESTS

Different types of Pd-Ag membranes have been tested at different operating conditions. The types of membranes tested are conventional ceramic and metallic supported and ultra-thin ceramic supported membranes. Table 1 shows the details of the membranes tested in terms of N_2 permeance at room temperature, time of plating, length**,** support size, H_2 permeance at 400 ºC for pure gas tests. The membrane E722, is an exception since it has been tested at 300 ºC, more details on this will be given in the next section. Figure 2. shows the ultra-thin Pd-Ag membranes E633 with 10/7 support and E737 with 14/7 support, the metallic supported membrane E681 and the membrane E722 ceramic supported brazed to a metallic tube.

Table 1. Description of the membranes tested

Code	Thickness [µm]	Support size [mm]	Ideal permselectivity H_2/N_2 (1bar)@400 ºC	Hydrogen permeance $*10^{-6}$ [mol/s/m^2/Pa] at 1 atm
E633	1.5	10-7	580	6.27
E635	1.3	10-7	252	7.7
E689	0.8	10-7	433	7.78
E681*	3-5	10-7	12056	1.99
E682*	3-5	10-7	1034	1.33
E642	3-5	10-4	21934	2.07
E582	3-5	10-7	1404	1.22
E737	2-3	14-7	2428	1.49
E738	2-3	14-7	731	2.2
E741A	2-3	10-7	13776.5	5.8
E722	4-5	10-9	>1386000	0.5**

*Metallic support sealed with graphite gaskets
** Tested at 300 ºC

The membranes have been tested by changing the pressure, the hydrogen molar fraction and the type of mixture in order to evaluate the influence on the hydrogen recovery factor and purity. Moreover, the focus has been kept on reproducing the operating conditions of the HyGrid system in order to evaluate the hydrogen flow rate recovered.

After the membrane was installed in the reactor, nitrogen was fed to check leakages and to measure the N_2 permeation at room temperature. Then, the heat up procedure was started in order to reach the temperature required for starting the activation of the membrane. The N_2 is measured while heating the reactor to understand if the leakage decreases according to Knudsen diffusion or if the sealing is failing due to high temperature. The N_2 permeance decreased with the temperature because of Knudsen diffusion meaning the main defects are

smaller than 50 nm. Once the reactor reaches the temperature, the membrane is activated with air for 2 minutes. Pure H_2 and N_2 permeation are measured before and after the activation at different pressure difference between the retentate and the permeate.

Figure 2. The membrane E722 is depicted in the top left, membrane E633 in the top right and membrane E737 in middle, metallic supported membrane E681 in the left bottom and E736a, E736b and E741a in the bottom right

Once the H_2 permeation became stable, pure gas tests were performed at different temperatures and pressure in order to calculate the activation energy, the pre-exponential factor and the exponent to be able to apply the Sieverts' law. In Figure 3 the trend of H_2 flux is plotted with the temperature while in Figure 4, the selectivity trend with the temperature is shown for the membrane E635. As the H_2 flux is related to the temperature as depicted in equation (1), when the temperature increases, the H_2 flux increases.

$$J_{H2} = Q * \left(p_{H2ret}^{n} - p_{H2perm}^{n}\right) * A \qquad (1)$$

In which, Q is the permeance in [mol/s/m^2/Pa^n], p_{H2ret}^n is the partial pressure of hydrogen at the retentate side at the power n, which is the exponent, A is the area of membrane. The selectivity decreases with the pressure because the H_2 depends on the partial pressure with an exponent lower than 1, while the impurities are directly linear with the partial pressure.

When the temperature increases, the selectivity increases because the H_2 flux increases according to equation (1), while the impurities permeation decreases because of Knudsen diffusion as it is possible to see in Figure 5. The selectivity has been calculated as ratio between pure H_2 and pure N_2 at the same partial pressure. In the case of a different gas, such as CH_4, the selectivity will change.

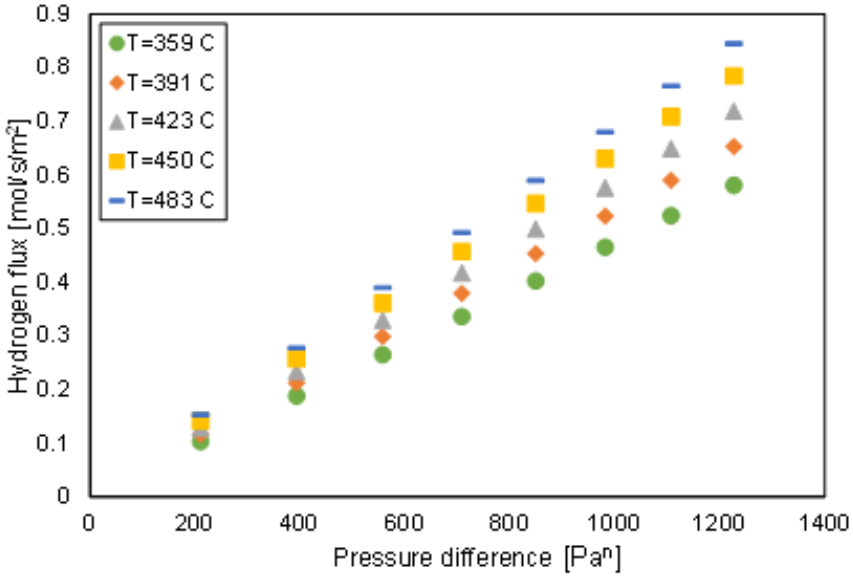

Figure 3. Plot of H_2 flux with the temperature

It depends on the size of the defects. If it is lower than 50 nm, Knudsen diffusion takes place which is related to the molecular weight of the gases.

The membrane E635 has been tested to check the influence of different gases on the selectivity. The table 2 describes the results obtained for pure gas when the retentate pressure has been changed from 5 to 2 bar while the permeate pressure was equal to 1 bar. The permselectivity obtained are close to those calculated from Knudsen (are 2.1 and 2.6 for He/CH_4 and H_2/N_2 respectively) which indicate that most of the defects are below 50 nm. As can be seen, the He flux is higher compared to N_2 or methane because of the lower molecular weight.

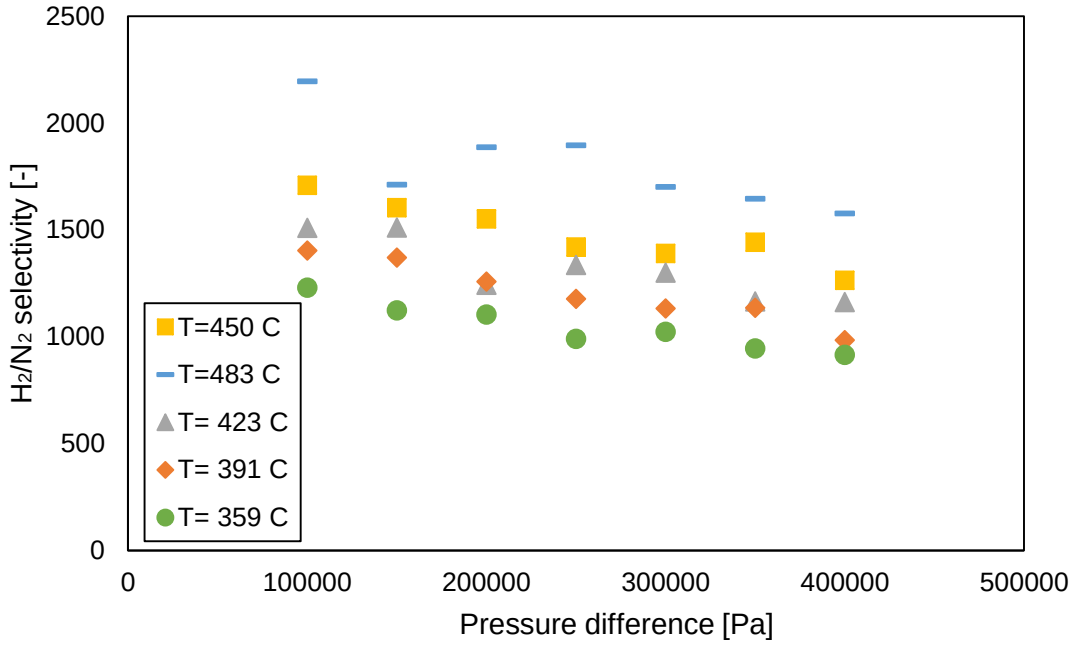

Figure 4. Plot of the selectivity with the pressure at different temperature

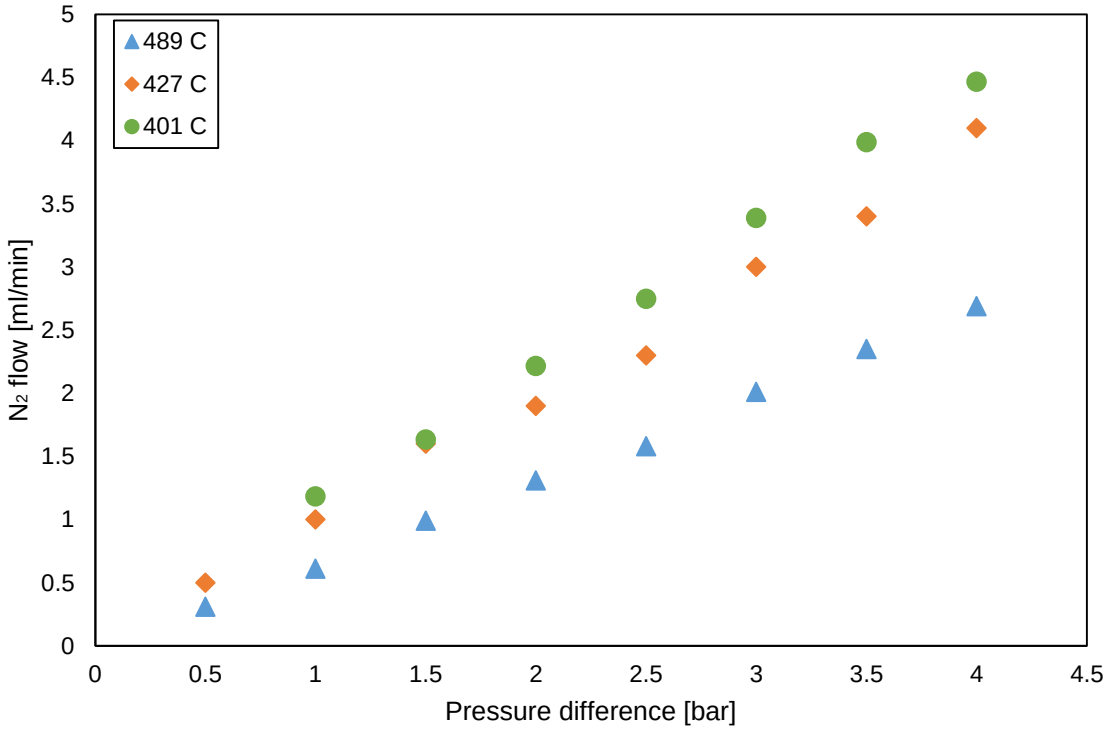

Figure 5. Trend of the impurities with the temperature for membrane E582

Table 2. He, CH_4 and N_2 flux at various pressure differences at 400 °C for membrane E635

ΔP / bar	Flux / mol s^{-1} m^{-2}			Perm selectivity	
	He	CH_4	N_2	He/CH_4	He/N_2
4.0	0.0030	0.0017	0.0013	1.8	2.3
3.5	0.0025	0.0014	0.0011	1.8	2.3
3.0	0.0020	0.0012	0.0009	1.7	2.2
2.5	0.0018	0.0010	0.0008	1.8	2.3
2.0	0.0014	0.0008	0.0006	1.8	2.3
1.5	0.0012	0.0006	0.0004	2.0	3.0
1.0	0.0008	0.0004	0.0003	2.0	2.7

Table 3. Exponent values of the membranes tested

	Thickness [µm]	Exponent [-]
E633	1.5	0.60
E635	1.3	0.65
E689	0.8	0.68
E681*	3-5	0.51
E682*	3-5	0.55
E642	3-5	0.53
E582	3-5	0.58
E737	2-3	0.60
E738	2-3	0.61
E741A	2-3	0.67
E722	4-5	0.79

The values of the exponent have been depicted in Table 3. The main observation is related to the ultra-thin membranes E633, E635 and E689, since the value of n is higher than 0.5. Usually, the diffusion through the membrane layer is the rate limiting step and the hydrogen permeation through the membrane can be described by the Sievert's law but, when the membrane becomes thinner, the diffusion through the membrane bulk becomes more rapid and another step might limit the permeation rate. The support could also play an important role since for membranes E737 and E738, the exponent is higher than 0.5. It means the diffusion through the bulk is not the rate limiting step but probably the support is also limiting.

In all the membrane tests, especially for the ultra-thin, the exponent was higher than 0.5. It means the hydrogen flux does not depend only on atomic diffusion through the palladium but it

is also influenced by kinetic of hydrogen splitting, the resistance of passage of gas H2 by the support and other factors such as the presence of impurities on the membrane surface.

Furthermore, the influence of the sweep gas in presence of mixtures has been studied to understand the behaviour of the hydrogen recovery and purity when the HyGrid conditions have been applied. At the beginning the amount of nitrogen as sweep gas was increased to study the H_2 flux in a mixture of 10% H_2 and 90% CH_4 similar to the operating condition of the HyGrid project. As can be seen in figure 6, the sweep gas is having a positive influence until an upper value, above which it is not possible to reduce the permeate pressure and increase the driving force. In Figure 6 the results depicted are referred to the metallic supported membrane E681. The operating conditions are 5 l/min of flow rate with 90% CH_4 and 10% H_2. The gas used for the sweep gas is nitrogen. The temperature is 400 C while the pressure has been changed from 5 bar to 1.5 bar in the retentate side and 1 bar in the permeate side. The hydrogen recovery factor (HRF) is the ratio between the hydrogen flux permeated and the hydrogen fed in the retentate side. It is important to underline the HRF increases up to 2 l/min of sweep gas, but from 3 to 5 l/min the HRF decreases; this behaviour could be attributed to the higher mass transfer limitation in the permeate side or in the porous support for higher sweep gases. Indeed, at the same partial pressure, in case of 2 l/min of sweep gas, the hydrogen flux permeated is higher compare to the case of 5 l/min as sweep gas.

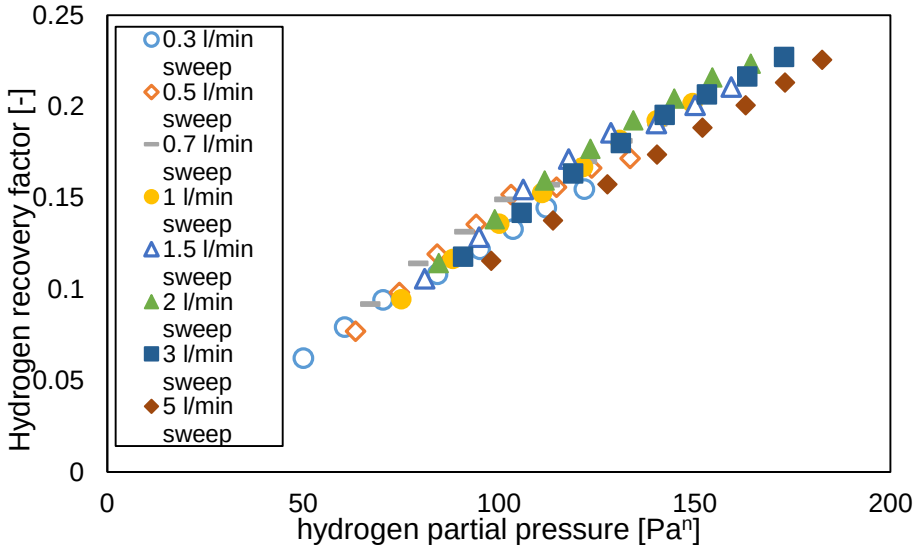

Figure 6. Hydrogen recovery factor with the partial pressure changing the amount of sweep gas

The main explanation for the reduction of hydrogen flux with higher sweep gas could be explained by higher partial pressure of hydrogen at the interface between the palladium and the

porous support. The higher partial pressure is due to the lower sweep gas fraction that is able to reach the surface of the palladium because of a pressure drop in the porous support. Moreover, the type of sweep gas has been changed to understand if different gases could play a role in the hydrogen permeation. Different mixtures and sweep gases have been applied to perform the experiments. The results are depicted in Figure 7. The total flow rate in the feed is equal to 5 l/min while the sweep gas to 0.5 l/min.

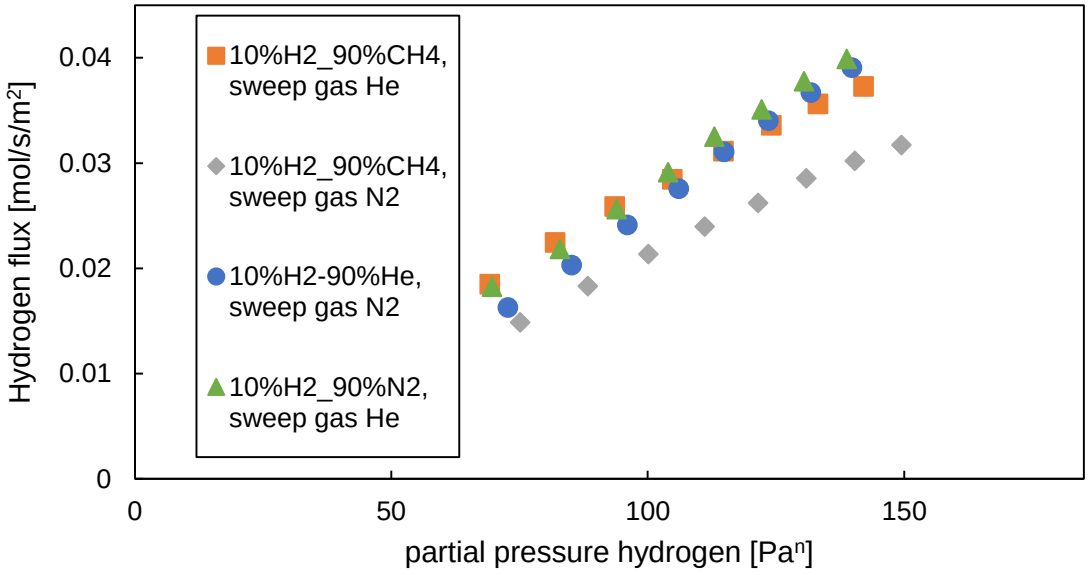

Figure 7. H_2 flux with the partial pressure changing the type of sweep gases and mixture

The main consideration from the experiments performed is related to the mass transfer limitation in the permeate side or porous support that is related to the binary diffusivity of H_2 in the sweep gas. These experiments have been performed to understand the behaviour of the hydrogen flux when different types of sweep gases have been used. Since in the HyGrid project the sweep gas is steam, it is important to study the behaviour of the HRF and purity when a different sweep gas is used because the tests have been performed without steam. The grey and the orange points are the trends for the H_2-CH_4 mixture with N_2 and He as sweep gas respectively. The diffusivity of H_2 in helium is almost twice the diffusivity of H_2 in nitrogen. It could explain the difference between the two trends in terms of HRF. The diffusivity of H_2 in steam is between the previous two, it means the line for a mixture with steam as sweep gas should stay in the middle between the grey and the orange.

Then, the influence of the sweep gas has been studied to understand if it is a real benefit for the driving force in terms of partial pressure. To perform this experiment, different H_2 molar fraction has been changed with and without sweep gas. Then the trend in case of sweep gas has been

compared to the results without sweep gas. The total flow rate is equal to 5 l/min while the total pressure in the retentate side has been changed from 5 bar to 2 bar. The main results are depicted in Figure 8, 9 and 10. In Figure 8 the results from a mixture of 90% CH_4 and 10% H_2 has been shown, in Figure 9 with 70% CH_4 and 30% H_2 while in Figure 10 with 50% CH_4 and 50% H_2.

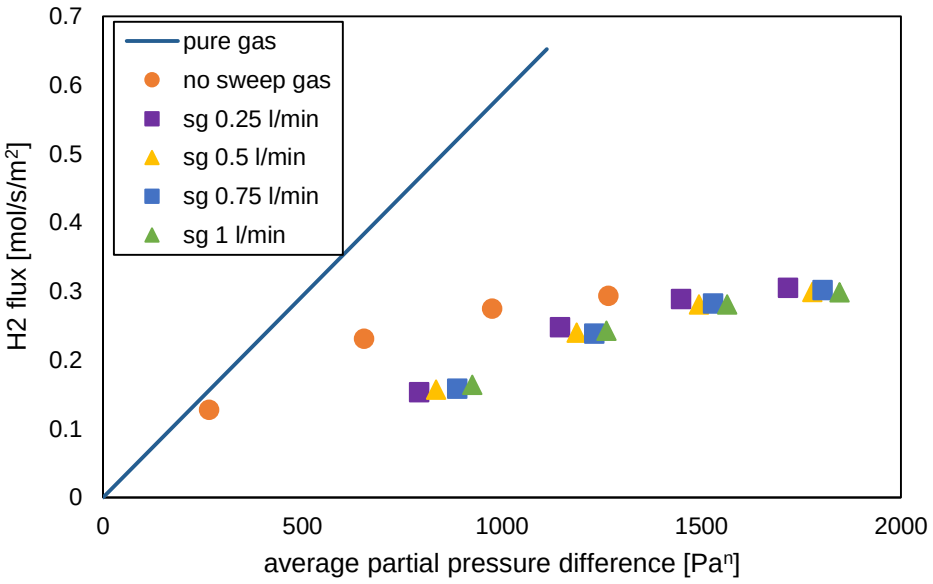

Figure 8. H_2 flux with the partial pressure with and without sweep gas for 90% H_2 and 10% CH_4 mixture

For all the results represented in Figure 8, 9 and 10, at the same partial pressure it seems convenient not to use sweep gas since the hydrogen flux is higher without sweep gas than with. The explanation could be found in the mass transfer limitation in the porous support. Actually the real driving force is not the one depicted in the Figure because the partial pressure difference takes into account only the ideal driving force without considering the mass transfer limitation. Moreover, for lower hydrogen concentration in the feed the distance between the hydrogen flux in the experiment without sweep gas is closer to the experiment with sweep gases. The mass transfer limitation in the porous support decreases in presence of lower hydrogen concentration in the retentate side.

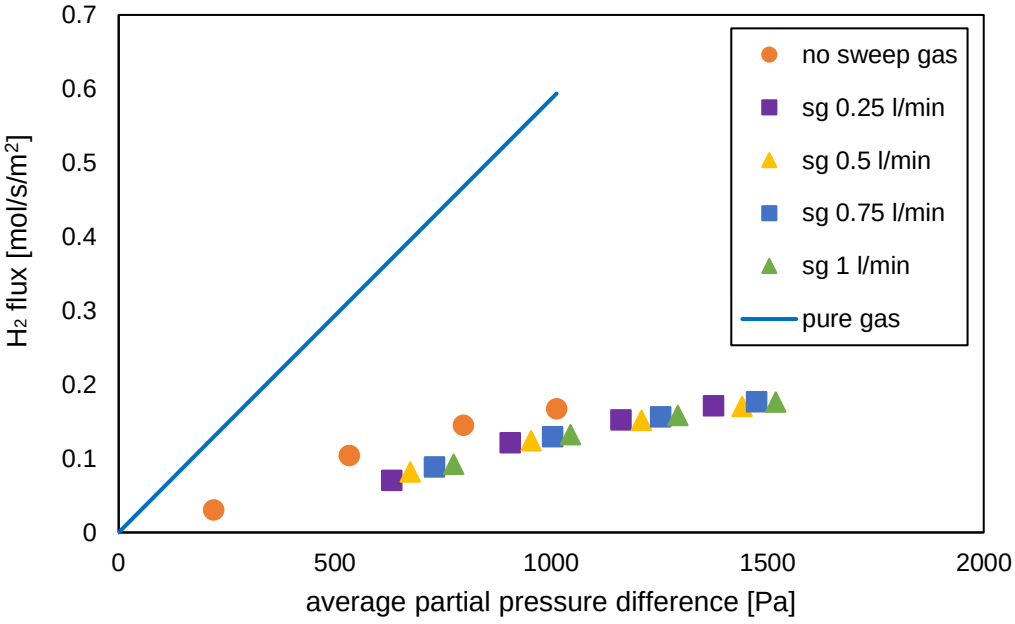

Figure 9. H_2 flux with the partial pressure with and without sweep gas for 70% H_2 and 30% CH_4 mixture

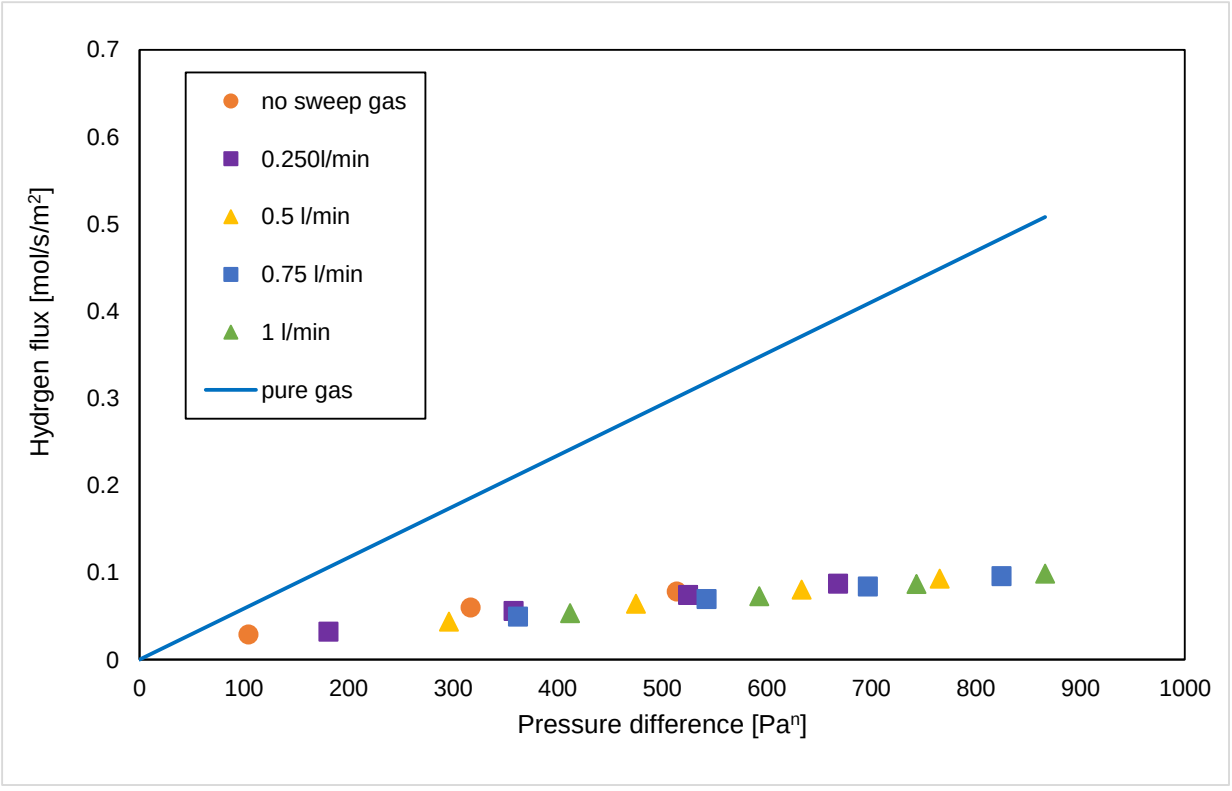

Figure 10. H_2 flux with the partial pressure with and without sweep gas for 50% H_2 and 50% CH_4 mixture

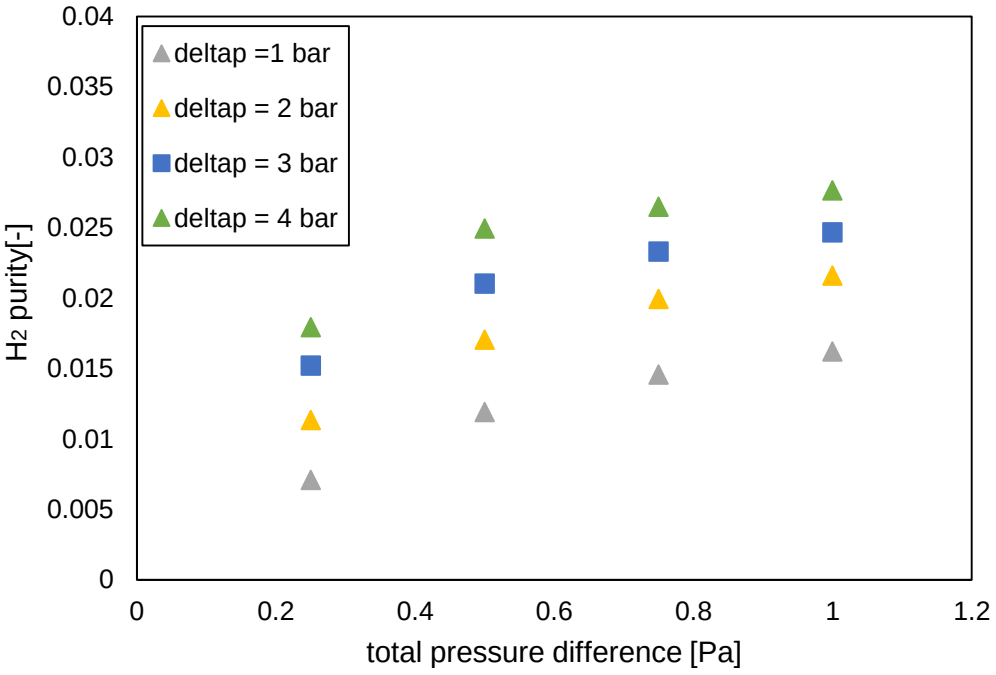

Figure 11. H_2 flux with the amount of sweep gas for different total pressure difference between retentate and permeate side

Considering the membrane E722, the ceramic support has been brazed to the metallic tube in SAES while the membrane has been prepared in TECNALIA and sent to TUE to perform permeation tests. In the reactor, the membrane was broken at the transition between the ceramic and the metallic part. In order to test anyway the H_2 permeation and the selectivity of the membrane, two caps have been used to cover the membrane and a black resin has been applied in order to avoid leakages. The membrane has been depicted in Figure 12.

After the membrane has been installed in the reactor, pure gas tests have been carried out for calculating the hydrogen permeability and the selectivity. When the membrane was installed in the reactor, N_2 permeation at room temperature has been checked to compare the broken membrane with caps to the original one. The value is higher compared to the original one. The N_2 permeation is equal to $9.38*10^{-11}$ mol/s/m^2/Pa. The reactor has been heated up at different temperatures and pressure while the hydrogen flow rate was measured. The permeability at 300 ºC was equal to $5*10^{-7}$ mol/s/m^2/Pa and the exponent to 0.79. The permeability is lower compared to conventional ceramic supported membrane because the porous support is symmetric and it is more difficult for gases to permeate than the asymmetric supports. When the membrane was heated up, the nitrogen impurities decreases. At 260 ºC the N_2 permeance was equal to $3.7*10^{-11}$ mol/s/m^2/Pa. At higher temperature the N_2 could not be measured anymore. The selectivity at 5 bar in the retentate and 1 bar in the permeate has been considered higher

than 1380000 N_2 could not be measured with the manual flow meter for small flow rate. The minimum detection is equal to 0.0001 ml/min. The value is much higher compare to the conventional ceramic supported membrane. A SEM picture of the porous support has been shown in Figure 13.

Figure 12. Membrane E722 sealed with two caps and black resine

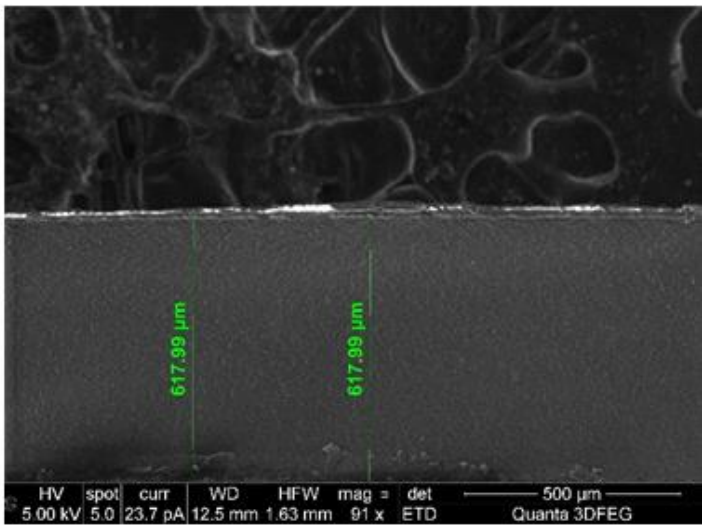

Figure 13. SEM analysis of membrane E722

5. MEMBRANE MODEL

5.1 Sieverts'law

In order to simulate the membrane, a model has been developed. It divides the Pd-Ag membranes into 150 cells and it applies the Sievert's law in each cell in order to calculate the permeated flux.

$$J_{H2} = P_m \left(p_{H2ret}^n - p_{H2perm}^n\right) A \qquad (1)$$

In which, P_m is the hydrogen permeance, p_{H2ret}^n , p_{H2perm}^n are respectively the partial pressure of hydrogen at the retentate and permeate side at the power n, which is the exponent. A is the membrane area. The permeance is obtained from the Arrhenius law:

$$P_m = P_0 e^{-\frac{E_a}{RT}}$$

Where the P_0 is the pre-exponential, E_a the activation energy and T is the membrane temperature. The enter parameters are the total volumetric flow rate, the hydrogen concentration, the feeding and permeate absolute pressures, the operating temperature, the permeability of hydrogen, the permeability of the impurities, the exponent of the Sievert's law and the area of the membrane.

5.2 Mass transfer limitation in the retentate side

A model for the simulation of the membrane has been developed in this work in order to account for the mass transfer limitation in the retentate, porous support and permeate side. The mass transfer limitation on the retentate side is mainly due to the lower hydrogen concentration on the palladium surface compare to the bulk. In presence of mixture, such as CH_4, the high rates of H_2 permeation through Pd membrane results in an accumulation of CH_4 and a depletion of H_2 in the boundary layer near the surface of the membrane. The partial pressure at the retentate side could be estimated from a Sherwood correlation which allow the calculation of the mass transfer coefficient for the mixture considered. The Maxwell-Stephan equation has been considered for taking into account multi-components system. The stagnant-film model is described by the sum of molecular and convective contributions to the mass flux as it is possible to see in equation (2).

$$N_{H_2} = J_{H_2} + x_{H_2} \sum_{i=1}^{N} N_i \qquad (2)$$

To achieve a better estimation of the partial pressure of hydrogen at wall, the zero rate mass transfer coefficient, is adjusted for a non-zero flux. The correction is based on the stagnant-film

model. With the stagnant-film model and the Fick's law, the partial pressure of hydrogen at the membrane surface was estimated based on the bulk phase pressure and zero mass transfer coefficient. The flux computation is divided into two parts. First, the concentration, flux and mass transfer coefficient at the interface between the bulk and the boundary layer are calculated. Then, the same method has been used for calculating the concentration at the membrane wall and the correction factor for the permeation through the membrane wall. When only the hydrogen flux is considered, as stated in equation (3) and the Fick's law (4) is considered, it is possible to derive equation (5). The continuity equation states the flux does not change at steady state according to equation (6). While equation (7) is obtained integrating twice equation (6).

$$\sum_{i=1}^{N} N_i = N_{H_2} \tag{3}$$

$$J_{H_2=} - cD_{H_2B}\frac{\partial x_{H_2}}{\partial y} \tag{4}$$

$$N_{H_2} = \frac{-cD_{H_2B}}{1 - x_{H_2}}\frac{\partial x_{H_2}}{\partial y} \tag{5}$$

$$\frac{\partial N_{H_2}}{\partial y} = \frac{\partial}{\partial y}\left(\frac{-cD_{H_2B}}{1 - x_{H_2}}\frac{\partial x_{H_2}}{\partial y}\right) = 0 \tag{6}$$

$$cD_{H_2B}\ln\left(1 - x_{H_2}\right) = k_1 y + k_2 \tag{7}$$

k_1 and k_2 can be calculated from the following boundary conditions:

$$y = 0 \quad x_{H_2} = x_{H_{2,bulk}};\ \ k_2 = cD_{H_2B}\ln\left(1 - x_{H_{2,bulk}}\right)$$

$$y = R^* \quad x_{H_2} = x^*_{H_2};\ \ k_1 = \frac{cD_{H_2B}}{R^*}\ln\left(\frac{1 - x^*_{H_2}}{1 - x_{H_{2,bulk}}}\right)$$

Both constants are substituted in equation (8) and the equation can be rewritten in order to obtain x_{H_2} equation (9) is the differential form of equation (8). Equation (9) can be combined with in order to obtain (10).

$$x_{H_2} = 1 - \left(1 - x_{H_{2,bulk}}\right)\left[\frac{1 - x^*_{H_2}}{1 - x_{H_{2,bulk}}}\right]^{\frac{y}{R^*}} \tag{8}$$

$$\frac{\partial x_{H_2}}{\partial y} = -\frac{1 - x_{H_{2,bulk}}}{R^*}\left[\frac{1 - x^*_{H_2}}{1 - x_{H_{2,bulk}}}\right]^{\frac{y}{R^*}} \ln\left[\frac{1 - x^*_{H_2}}{1 - x_{H_{2,bulk}}}\right] \quad (9)$$

$$N_{H_2} = \frac{cD_{H_2B}}{R^*}\frac{1 - x_{H_{2,bulk}}}{1 - x_{H_2}}\left[\frac{1 - x^*_{H_2}}{1 - x_{H_{2,bulk}}}\right]^{\frac{y}{R^*}} \ln\left[\frac{1 - x^*_{H_2}}{1 - x_{H_{2,bulk}}}\right] \quad (10)$$

When the molar fractions are rewritten into partial pressure and the mass transfer coefficient, $k_g$is considered $\frac{D_{H_2B}}{R^*}$, equation (11) is found.

$$N_{H_2}|_{y=R^*} = k_g cln\left[\frac{P - P^*_{H_2}}{P - P_{H_{2,bulk}}}\right] = Q\left(P^{*n}_{H_2} - P^{*n}_{H_2,perm}\right) \quad (11)$$

For the calculation of the mass transfer coefficient in the retentate side, a Sherwood correlation has been used. It is available for developed velocity and concentration profiles (Nu_∞, Sh_∞) as a function of the ratio of annular radii. The correlation used in this work is described in equation (12).

$$Sh = Sh_\infty = 6.18, for\ Gz \leq 62 \quad (12)$$

From equation (11) it is possible to estimate the mass transfer coefficient from equation (13).

$$Sh = \left(k_{g,ret} * \frac{d_{eq}}{D_{H2}}\right) \quad (13)$$

After the concentration polarization has been implemented in the retentate side, the model has been validated with experimental results in which binary mixtures have been tested.

After the concentration polarization has been implemented in the retentate side, the model has been validated with experimental results in which binary mixtures have been tested.

In Figure 14, it is possible to see the results obtained in the comparison between experimental results and modelling including mass transfer in the retentate side. From the results, the model seems able to predict the experimental tests.

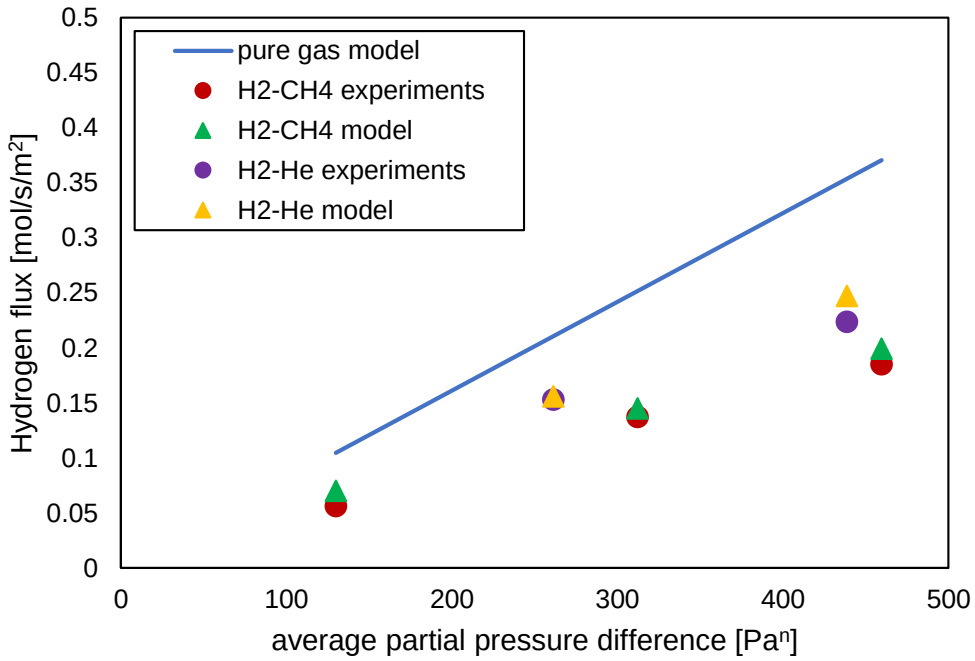

Figure 14. Comparison between experimental and modelling results for two different mixtures in case of 50% H_2 and total volume flow rate equal to 1 l/min

The red and purple points, described the experimental results, with a mixture, respectively of H_2-CH_4 and H_2-He in case of total flow rate of 1 l/min and inlet molar fraction of hydrogen of 50%. The green and yellow points are the simulation results respectively for hydrogen-methane and hydrogen-helium. Changing the partial pressure, the model is still able to predict the experimental results. The concentration polarization in the retentate side increases the molar fraction of the other gas of the mixture that is not hydrogen compared to the bulk. As it is possible to visualize in Figure 15, the difference in terms of molar fraction is remarkable and gives a high negative contribution to the driving force.

If the same equations described before, are applied for taking into account the concentration polarization in the permeate side, the model it is not able to predict the results for a mixture in presence of sweep gas. The results are shown in Figure 16. For this reason, the difference in terms of molar fraction between the bulk and the surface of the permeate side is not relevant. It means the contribution of concentration polarization is negligible while it is important to study more in details the influence of the porous support in presence of sweep gas.

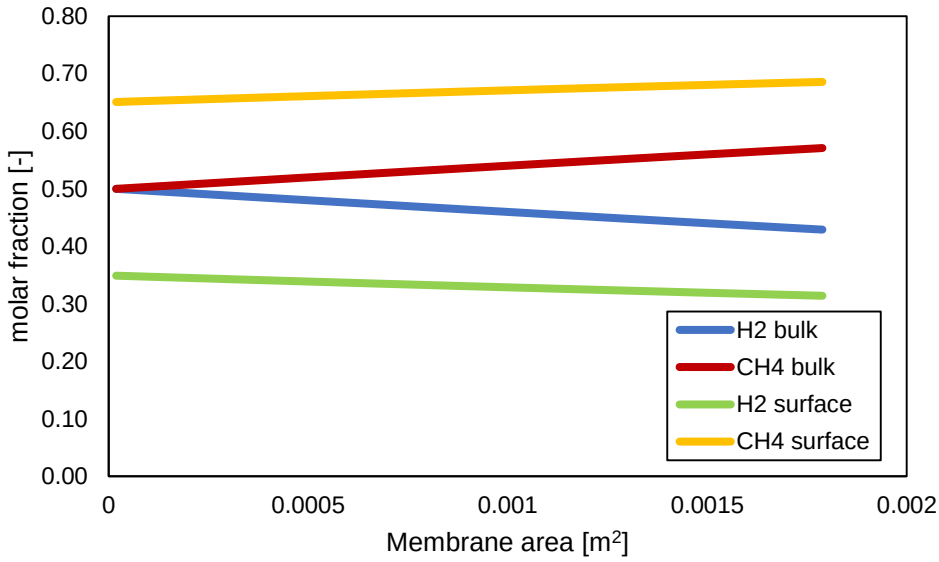

Figure 15. Trend of the molar fraction in presence of mass transfer limitation in the retentate side for a mixture of hydrogen and methane

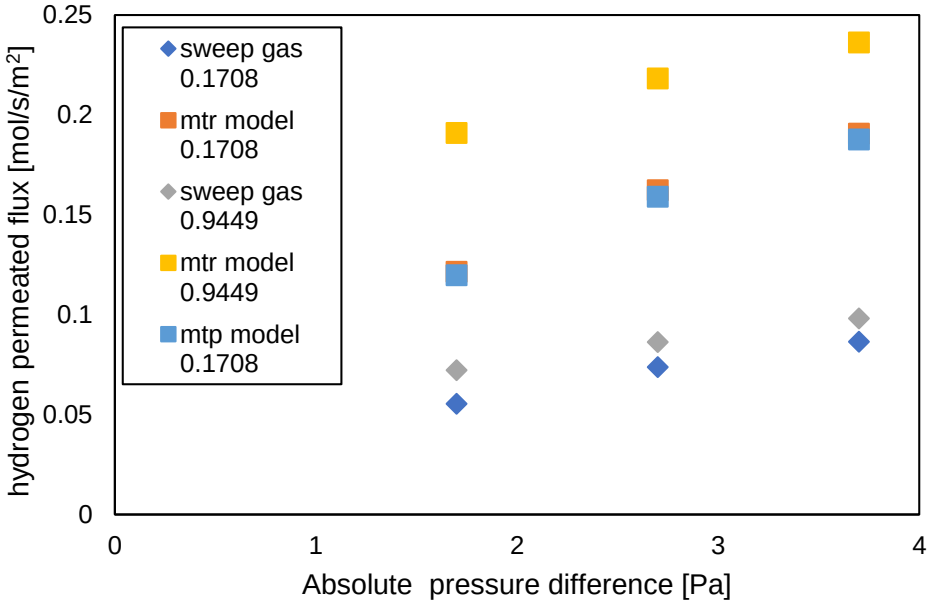

Figure 16. Comparison between experimental results in presence of sweep gas in a mixture of 50% H_2-50% CH_4 and simulations

The mass transfer limitation in the porous support is due to molecular friction resistance and a support friction resistance. In order to be able to describe properly, the dusty gas model has

been used to take into account the Knudsen diffusion flow (first term), the viscous flow (second term) and the binary diffusion (third term).

Once the mixture reaches the Pd layer, only hydrogen can be permeating due to the high selectivity. When nitrogen is used as sweep gas, in the permeate side, the membrane sees the mixture of hydrogen and nitrogen. The equation of the dusty gas model has been written for the specie of hydrogen and for the specie of nitrogen. Considering stagnant gas in the porous support, the flux of nitrogen could be considered equal to zero. If equation (11) and (12) are summed up, it is possible to obtain equation (13).

5.3 Concentration polarization in the permeate side

In order to consider the concentration polarization in the permeate side, the equation (6) has been integrated for the permeate side as it is possible to see in equation (14).

$$N_{H_2}|_{y=R^*} = k_{g,perm} cln\left[\frac{P - P_{H_{2,permbulk}}}{P - P^*_{H_{2,perm}}}\right] = Q\left(P^{*n}_{H_2} - P^{*n}_{H_{2,perm}}\right) \quad (14)$$

In which the mass transfer coefficient $k_{g,perm}$ is calculated from a Sherwood correlation for internal convention as described in equation (15).

$$Sh = Sh_\infty = 5.04, for\ Gz \leq 51 \quad (15)$$

The final system that has been considered in order to take into account the mass transfer limitation in retentate and permeate is equal to system (16).

$$\begin{cases} N_{H_2}|_{y=R^*} = k_{g,ret} cln\left[\dfrac{P - P^*_{H_{2,ret}}}{P - P_{H_{2,retbulk}}}\right] = Q\left(P^{*n}_{H_{2,ret}} - P^{*n}_{H_{2,perm}}\right) \\ N_{H_2}|_{y=R^*} = k_{g,perm} cln\left[\dfrac{P - P_{H_{2,permbulk}}}{P - P^*_{H_{2,perm}}}\right] = Q\left(P^{*n}_{H_2} - P^{*n}_{H_{2,perm}}\right) \end{cases} \quad (16)$$

Where the mass transfer coefficient in the retentate and permeate side, are estimated as explained before.

5.4 Mass transfer limitation in the porous support

The mass transfer limitation in the porous support is due to molecular friction resistance and a support friction resistance. In order to be able to describe it properly, the dusty gas model,

depicted in equation (17) has been used to take into account the Knudsen diffusion flow (first term), the viscous flow (second term) and the binary diffusion (third term).

Once the mixture reaches the palladium layer, only hydrogen can permeating due to the high selectivity. When nitrogen is used as sweep gas, in the permeate side, the membrane see the mixture of hydrogen and nitrogen. The equation of the dusty gas model has been written for the specie of hydrogen and for the specie of nitrogen. Considering stagnant gas in the porous support, the flux of nitrogen could be considered equal to zero. If equation (17) and (18) are summing, it is possible to obtain equation (19).

$$-\frac{1}{RT}\frac{dP_2}{dz} = \frac{1}{D_{K1}}\left[N_2 + x_2 B_0 \frac{P}{\mu RT}\frac{dP}{dz}\right] + \frac{x_1 N_2 - x_2 N_1}{D_{12}} \quad (17)$$

$$-\frac{1}{RT}\frac{dP_1}{dz} = \frac{1}{D_{K1}}\left[N_1 + x_1 B_0 \frac{P}{\mu RT}\frac{dP}{dz}\right] + \frac{x_2 N_1 - x_1 N_2}{D_{12}} \quad (18)$$

In which B_0 is the viscous permeability of the support matrix, D_{K1} is the Knudsen diffusivity for specie one, D_{12} is the binary diffusivity, N_1 and N_2 are respectively the flux of hydrogen and nitrogen.

$$N_1 = -\frac{D_{K1}}{RT}\left(1 + \frac{B_0 P}{\mu D_{KA}}\right)\frac{dP}{dz} \quad (18)$$

In which,

$$(D_{KA}) = \frac{x_1}{D_{K1}} + \frac{x_2}{D_{K2}}$$

Substituting equation (19) in equation (18) and integrating, it is possible to find equation (20) which described the pressure difference in the porous. It is function of the total pressure at the retentate side, the hydrogen concentration at the bulk of the permeate side, the average pressure on the porous support and the characteristics of the support. The main parameters of the support are the porosity, the tortuosity and the pore size.

$$\Delta P = P(L) - P(0) = -\frac{ln\left[\frac{1-x_1(L)}{1-x_1(0)}\right]}{\frac{D_{K1}}{D_{12}^0} + \frac{B_0}{\mu D_{K2}} + \frac{B_0}{\mu D_{KA} D_{12}^0} P D_{K1} + \frac{1}{P}} \quad (20)$$

The effective Maxwell-Stefan gas-gas diffusivity in a porous support is given by

$$D_{ij}^0 = \frac{\varepsilon}{\tau} D_{ij}$$

Where ε and τ are the porosity and the tortuosity of the ceramic porous support respectively and D_{ij}^0 is the Maxwell-Stefan gas-gas diffusivity which is equal to the Fick diffusivity for an ideal gas. The effective Knudsen diffusivity is given by:

$$D_{Ki} = \frac{\varepsilon}{\tau} \frac{d_{pore}}{3} \sqrt{\frac{8RT}{\pi M_i}}$$

Where d_{pore} is the pore diameter and M_i is the molar mass of species i. If convection through the support is modelled as laminar, incompressible flow through cylindrical pores, the Hagen-Poiseuille law with added porosity and tortuosity modification gives:

$$B_0 = \frac{\varepsilon}{\tau} \frac{d_{pore}^2}{32}$$

Combining equation (19) and the corresponding equation for species 2, it is possible to obtain equation (21).

$$-\frac{D_{12}}{D_{K1}} \frac{P}{x_2} \frac{dx_2}{dz} = \frac{dP}{dz}\left[1 + \frac{D_{12}}{D_{K1}} + \frac{B_0 P}{\mu}\left(\frac{1}{D_{KA}} + \frac{D_{12}}{D_{K2} D_{K1}}\right)\right] \quad (21)$$

Then the term $\frac{dP}{dz}$ can be eliminated between equation (21) and equation (19).

If then it is integrated it is possible to find equation (22) in which the hydrogen flow depends on the hydrogen concentration at the surface, at the bulk of the permeate, on the average pressure along the porous support.

$$N_1 = \frac{P}{RTL} ln\left[\frac{1-x_1(L)}{1-x_1(0)}\right]\left[\frac{1}{D_{12}} + \frac{1}{D_{K1}} \frac{1 + B_0 P D_{KA}}{1 + B_0 P D_{K2}}\right]^{-1} \quad (22)$$

Combining equation (14) and (18), it is possible to solve the system and calculate partial pressure of hydrogen at the retentate side, pressure drop of the porous support and hydrogen concentration on the palladium surface at the permeate side.

$$\begin{cases} \dfrac{P - P^*_{H2,ret}}{P - P_{H_2\,bulk}} = \exp\left[\dfrac{Q}{ckg_{ret}}\left(P^{*n}_{H2,ret} - \left(\left(P_{tot\,perm} + \Delta P\right)x^*_i\right)^n\right)\right] \\ N_1 = \dfrac{P}{RTL} ln\left[\dfrac{1 - x_1(L)}{1 - x_1(0)}\right]\left[\dfrac{1}{D_{12}} + \dfrac{1}{D_{K1}}\dfrac{1 + B_0 P D_{KA}}{1 + B_0 P D_{K2}}\right]^{-1} \\ \Delta P = P(L) - P(0) = -\dfrac{ln\left[\dfrac{1 - x_1(L)}{1 - x_1(0)}\right]}{\dfrac{D_{K1}}{D^0_{12}} + \dfrac{B_0}{\mu D_{K2}} + \dfrac{B_0}{\mu D_{KA} D^0_{12}} P D_{K1} + \dfrac{1}{P}} \\ N_{H_2}|_{y=R^*} = k_{g,perm} c ln\left[\dfrac{P - P_{H_2,permbulk}}{P - P^*_{H_2,perm}}\right] = Q\left(P^{*n}_{H_2} - P^{*n}_{H_2,perm}\right) \end{cases}$$

All the membranes analysed have porous alluminia supports. In order to discover the support's limiting pore size distribution, a porosimetry test has been performed. In fact, the pinholes on the Pd-Ag membrane can be due to the structure of the porous support, which can allow a proper deposition of the selective layer or not. First of all, the leakages of the dry porous support are measured as a function of the absolute pressure difference across it. In this way it is possible to draw the so called dry line. To measure the leakages, the support is put in the reactor at ambient temperature. Then pure nitrogen is fed in the retentate at different absolute pressures and the permeated flux is measured at 1 bar. The second step is to immerse the support in a liquid, in the specific case ethanol has been used. The lower the surface tension of the liquid, the lower the pore size that can be measured at the same pressure level.

After 10 min the porous support is put again in the reactor and the measurement of the leakages is performed as before. With low absolute pressure differences no flux is detected, depending on the ethanol covered pores size that opens at different pressures. A new line can be drawn starting from the last measurements, the so called wet line. The distribution obtained has been depicted in Figure 17.

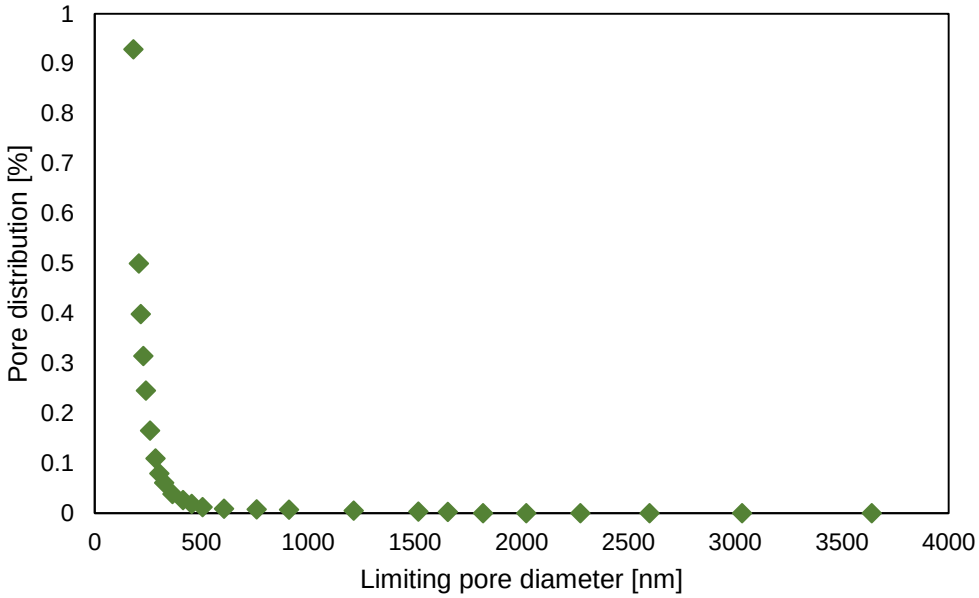

Figure 17. Pore distribution of the limitating pore diameter obtained from a porosimetry test for

Due to molecular and support friction, a pressure drop occurs on the porous support and the sweep gas is not able to reach the palladium surface. Moreover, the nitrogen direction is opposite to the hydrogen direction going from the palladium to the bulk of the permeate side. It promotes the pressure difference along the porous support. The ideal driving force for the permeation of hydrogen considers the bulk hydrogen concentration at the retentate side and the bulk hydrogen concentration at the permeate side. Since the sweep gas is not able to reach the palladium surface, the hydrogen concentration on the surface is higher compare to the bulk. The pressure drop on the porous support gives a negative effect on the pressure at the interface of the palladium surface causing a higher total pressure on the palladium surface compare to the total pressure of the bulk of the permeate side. It means the partial pressure on the surface at the permeate side is remarkably different compare to the partial pressure at the bulk in which all the sweep gas is mixed with the hydrogen separated. The main effect of the mass transfer limitation occurs in the retentate side even if the contribution of the porous support is important to be considered. In Figure 18 the partial pressure at the retentate bulk, retentate surface, permeate bulk and permeate surface have been depicted. It is important to notice the difference between the red and the yellow line gives information of the ideal driving force along the membrane area, while the difference between the blue and the green one, gives information on the real driving force that allow the hydrogen the permeate.

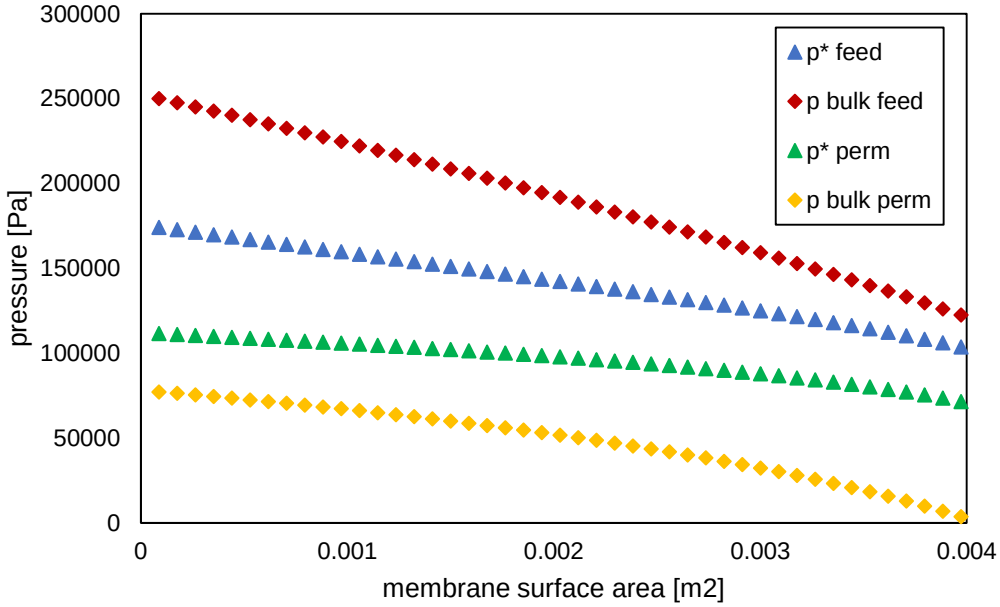

Figure 18. Bulk retentate pressure, surface retentate pressure, bulk permeate pressure and surface permeate pressure along the membrane area

In Figure 19, it is possible to visualize a SEM analysis of the porous support in order to understand the real distribution of the pore size. Only a small layer near the palladium layer, has a pore size of 100 nm while the entire support has a pore size distribution of 3 μm. The asymmetric support has the purpose to avoid mass transfer limitation in the support, which it could be visible in symmetric supports. The pore size considered in the simulation is a weighted average of the size near the palladium layer and the bigger pore size.

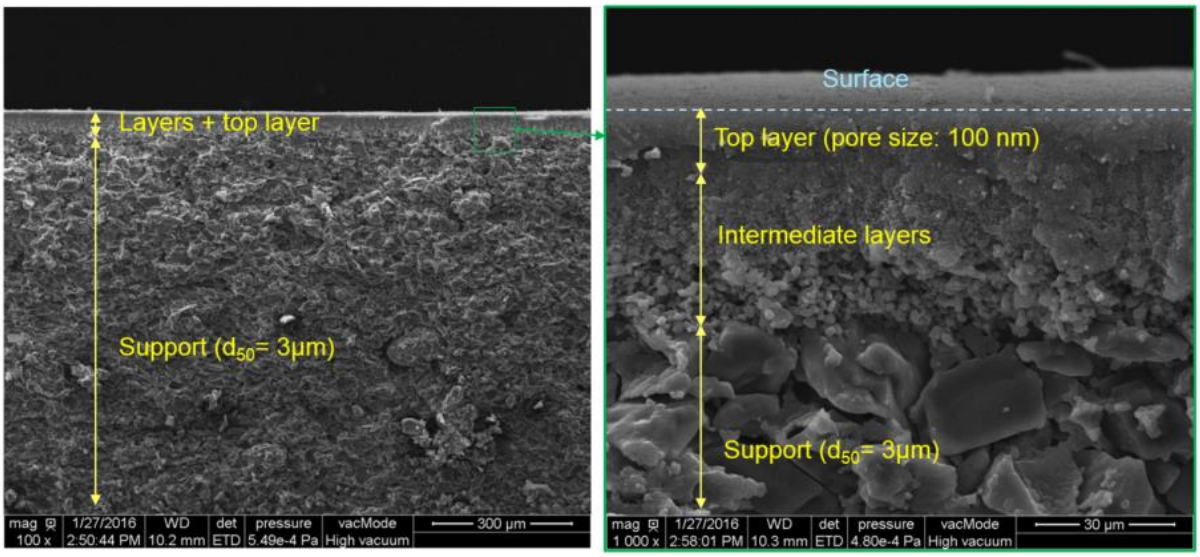

Figure 19. SEM analysis of the porous support

In Figure 20 and 21, it is possible to see the results obtained from the simulation compared to the experimental results. The operating conditions consist in a mixture of 50% H_2 50% CH_4 in the retentate side and 1 l/min for Figure 20, and 0.25 l/min for Figure 21, of sweep gas in the permeate side. Nitrogen has been used as sweep gas, while the total flow rate in the retentate side was equal to 1 l/min.

The yellow points describe the experimental results obtained with the described operating conditions. The blue points describe the simulation without mass transfer limitation. The orange points describe the simulation including only the mass transfer limitation in the retentate side. It is possible to realize the effect of concentration polarization in the retentate is remarkable. The green points are the results obtained from the simulation in which both the mass transfer limitation in the retentate and in the porous support are included. It is important to underline the mass transfer limitation in the porous support plays a relevant role in the experiments in presence of sweep gas, especially at high amount of sweep gas.

The reason for which the mass transfer limitation in the porous support is higher when the amount of sweep gas is increased, could be found in the higher pressure drop across the porous support. Even if the quantity of sweep gas that could reach the palladium layer, is higher at the same operating conditions, when more sweep gas is fed, the pressure at the interface increases and it results in higher or comparable partial pressure at the surface of the permeate side. It means there is an upper limit for which, increases the sweep gas, the driving force is not higher anymore.

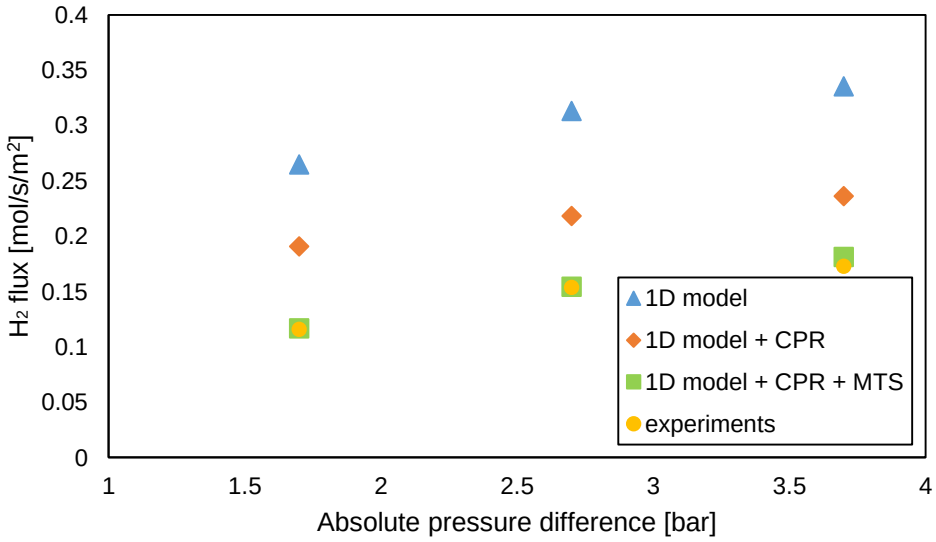

Figure 20. Comparison between experimental and modelling results for a mixture of CH_4-H_2 with nitrogen as sweep gas. The sweep gas is 1 l/min

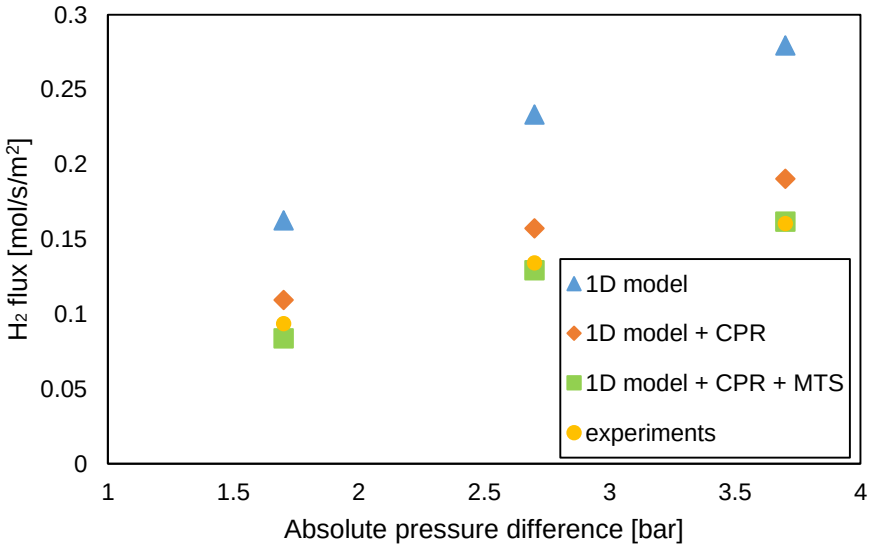

Figure 21. Comparison between experimental and modelling results for a mixture of CH_4-H_2 with nitrogen as sweep gas. The sweep gas is 0.25 l/min

6. SETUP FOR THE SORBENT TESTS

Different sorbents provided by Hygear have been tested in the University of Eindhoven in order to study the adsorption capacity by changing the flow rate, the partial pressure of steam and the temperature. The sorbents tested are zeolite 4A, modified zeolite 4A, zeolite 13X and silica gel. The setup consists of mass flow controllers up to 5 l/min to feed H_2 and N_2 and a mass flow controller to feed steam up to 30 g/h. The thermogravimetric analyser comprises a basket attached to a balance in order to measure constantly the weight change of the sample inside the basket. The picture of the setup and the schematic of the process flow diagram is shown in Figure 22, and 23 respectively.

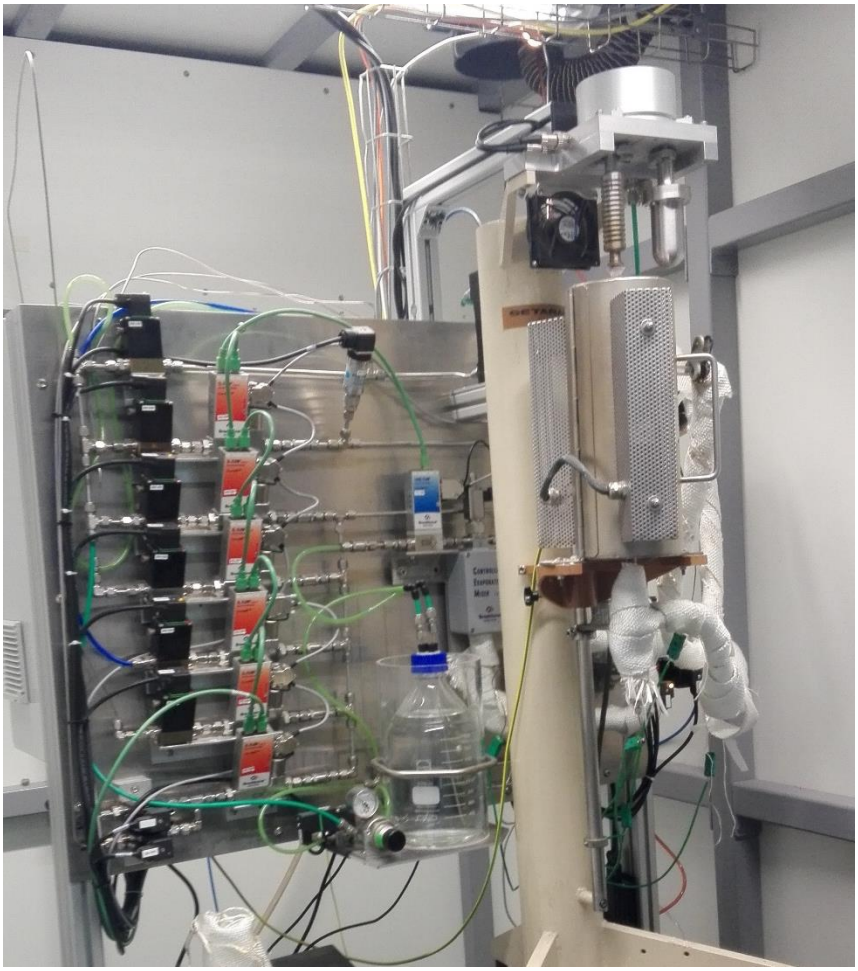

Figure 22. Picture of the thermogravimetric analysis setup

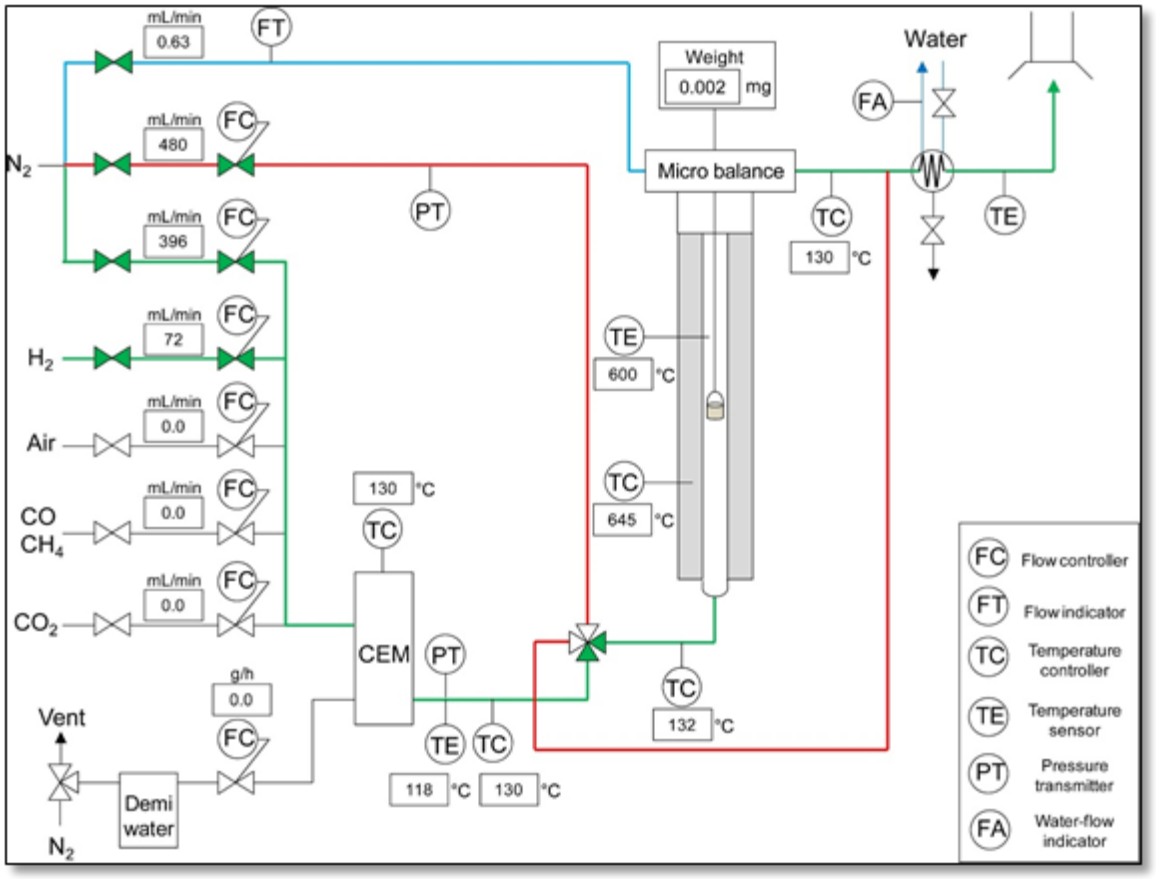

Figure 23. Schematic of the thermogravimetric analysis setup

7. SORBENTS TESTS

Before performing the experiments, the sample was loaded in the TGA and the balance was set to zero in order to be able to see the difference in weight when the experiment starts. Isothermal adsorption on zeolite 4A has been performed, as can be observed in Figure 24, changing the steam partial pressure, increasing the steam flow at different temperatures. As expected, the adsorption capacity increases at lower temperature following the Langmuir equation. Moreover, when the partial pressure of steam is higher, the adsorption capacity increases. In Figure 25, the results for silica are depicted. Comparing the results, it is possible to visualize quite a remarkable difference between the adsorption capacity of silica and zeolite. Zeolite has a double adsorption capacity compared to silica at the same temperature and partial pressure,

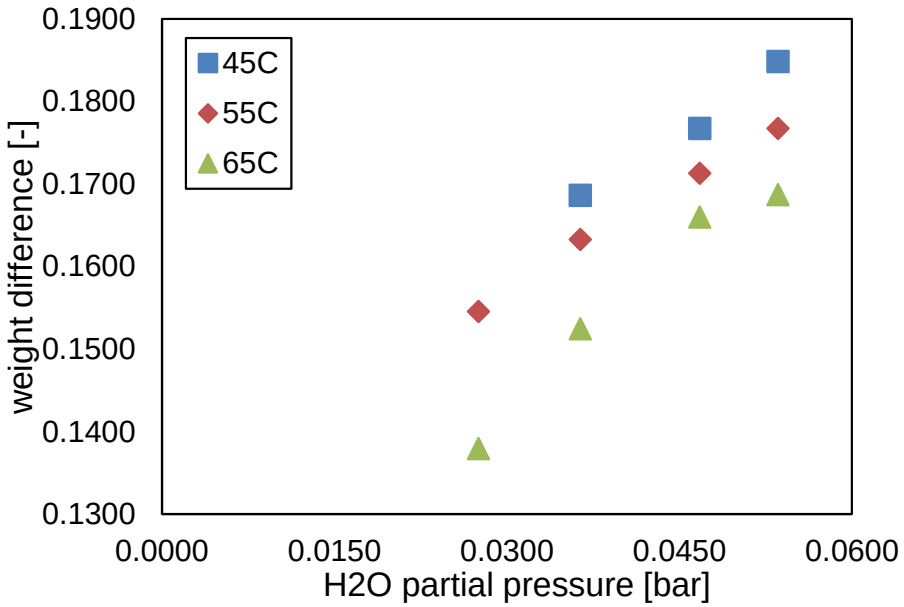

Figure 24. Isothermal adsorption changing steam pressure and temperature on zeolite 4A

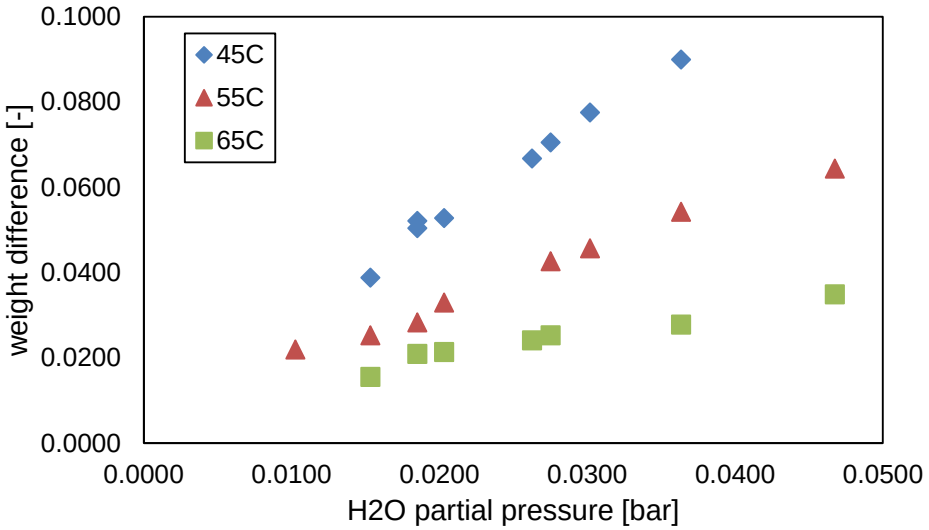

Figure 25. Isothermal adsorption changing steam pressure and temperature on silica beads

In Figure 26, it is possible to see the results for zeolite 13X. Its adsorption capacity is relatively better when compared to zeolite 4A. For the prototype the selection has been taken for zeolite 4A since the desorption of zeolite 13X is asking more heat consumption.

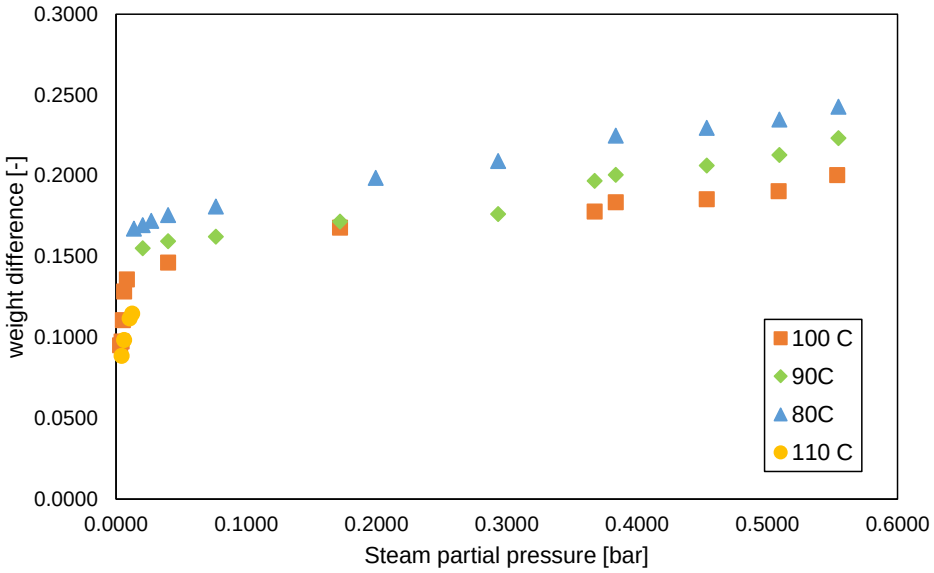

Figure 26. Isothermal adsorption changing steam pressure and temperature on silica beads

6. CONCLUSIONS

Different palladium membranes with different outer support diameter have been tested and simulated in presence of sweep gas for a proper understanding of the mass transfer role in the retentate, porous support and permeate side. A novel model for the prediction of the experimental results in presence of counter-current sweep gas has been developed. The main contribution to the mass transfer limitation in presence of sweep gas is the porous support. Pure gas tests and mixture tests have been performed before applying sweep gas in the permeate in order to be able to describe properly the concentration polarization in the retentate side. Once the validation of the model in presence of mixtures have been carried out, the study of the mass transfer limitation in the permeate side has been performed. The concentration polarization in the retentate side plays an important role in presence of mixture while when sweep gas is applied, the concentration polarization in the permeate side is negligible. Due to molecular and support friction, a pressure drop occurs on the porous support and the sweep gas is not able to reach the palladium surface. Moreover, the nitrogen direction is opposite to the hydrogen direction going from the palladium to the bulk of the permeate side. It promotes the pressure difference along the porous support. Since the sweep gas is not able to reach the palladium surface, the hydrogen concentration on the surface is higher compare to the bulk. The pressure drop on the porous support gives a negative effect on the pressure at the interface of the

palladium surface causing a higher total pressure on the palladium surface compare to the total pressure of the bulk of the permeate side. It means the partial pressure on the surface at the permeate side is remarkably different compare to the partial pressure at the bulk in which all the sweep gas is mixed with the hydrogen separated. Moreover this phenomenon becomes relevant for higher amount of sweep gas.

The main conclusion is the not so positive effect of the sweep gas due to the pressure drop in the porous support that does not allow the sweep gas to reach the interface between the palladium and the porous support. It means the driving force is lower compare to the expected one. Sorbent tests have been performed in order to select the best for the prototype. The zeolite 4A has been selected for the purpose because of its higher weight capacity and lower energy consumption required for the regeneration.

7. REFERENCES

[1] Pinacci, P., & Drago, F. (2012). Influence of the support on permeation of palladium composite membranes in presence of sweep gas. *Catalysis Today*, *193*(1), 186–193. https://doi.org/10.1016/j.cattod.2012.02.041

[2] Caravella, A., Barbieri, G., & Drioli, E. (2009). Concentration polarization analysis in self-supported Pd-based membranes, *66*, 613–624. https://doi.org/10.1016/j.seppur.2009.01.008

[3] Unal, A. (1987). Gaseous mass transport in porous media through a stagnant gas. *Industrial & Engineering Chemistry Research*, *26*(1), 72–77. https://doi.org/10.1021/ie00061a013

[4] Gorbach, A., Stegmaier, M., & Eigenberger, G. (2004). Measurement and Modeling of Water Vapor Adsorption on Zeolite 4A — Equilibria and Kinetics, 29–46.

[5] Gallucci, F., Fernandez, E., Corengia, P., & Sint, M. Van. (2013). Recent advances on membranes and membrane reactors for hydrogen production. *Chemical Engineering Science*, *92*, 40–66. https://doi.org/10.1016/j.ces.2013.01.008